NASA Technical Paper 2845

1988

Thermoviscoplastic Model With Application to Copper

Alan D. Freed
Lewis Research Center
Cleveland, Ohio

National Aeronautics and Space Administration

Scientific and Technical Information Division

Summary

A viscoplastic model is developed which is applicable to anisothermal, cyclic, and multiaxial loading conditions. Three internal state variables are used in the model: one to account for kinematic effects, and the other two to account for isotropic effects. One of the isotropic variables is a measure of yield strength, while the other is a measure of limit strength. Each internal state variable evolves through a process of competition between strain hardening and recovery. There is no explicit coupling between dynamic and thermal recovery in any evolutionary equation, which is a useful simplification in the development of the model. The thermodynamic condition of intrinsic dissipation constrains the thermal recovery function of the model.

Application of the model is made to copper, and cyclic experiments under isothermal, thermomechanical, and nonproportional loading conditions are considered. Correlations and predictions of the model are representative of observed material behavior.

Introduction

The design and development of advanced power systems require mathematical models capable of accurately predicting short-term plastic strain, long-term creep strain, and the interactions between them. Multiaxial, cyclic, and anisothermal loading states are normal service conditions, not exceptional ones. The main reason for doing inelastic analysis is not so much to determine the deformation response of a structure per se, but rather to assess its useful service life. Results from inelastic analyses are input to life assessing schemes. These schemes typically require such quantities as stress range, mean stress, inelastic strain range, and percentages of time-dependent creep and time-independent plasticity that make up the inelastic strain range (ref. 1). It is therefore of paramount importance that a viscoplastic model be capable of predicting these phenomena with reasonable accuracy.

The theoretical development of viscoplasticity has its origin with the works of Stowell (ref. 2), Prager (ref. 3), and Perzyna (ref. 4), whose models do not contain evolving internal state variables. The field experienced rapid advances in the 1970's when internal state variable models began to appear in the works of Geary and Onat (ref. 5), Bodner and Partom (ref. 6), Hart (ref. 7), Miller (ref. 8), Ponter and Leckie (ref. 9), Chaboche (ref. 10), Krieg et al. (ref. 11), and Robinson (ref. 12). Theoretical refinements have continued to occur throughout the 1980's in the models of Stouffer and Bodner (ref. 13), Valanis (ref. 14), Walker (ref. 15), Schmidt and Miller (ref. 16), Chaboche and Rousselier (ref. 17), Estrin and Mecking (ref. 18), Krempl et al. (ref. 19), Lowe and Miller (ref. 20), and Anand and Brown (ref. 21). Reviews on various aspects of viscoplasticity have been written by Perzyna (ref. 22), Walker (ref. 15), Chan et al. (ref. 23), Lemaitre and Chaboche (ref. 24), and Swearengen and Holbrook (ref. 25). Although this list is by no means complete, it is representative of the work done in viscoplasticity, and of the attention that it has received.

This report develops an anisothermal viscoplastic model applicable to polycrystalline metals. The concept of internal state variables is used, and the associated thermodynamic constraint of dissipativity is discussed. Three internal state variables are used in the model: one to account for kinematic hardening, and two to account for isotropic hardening. The evolutionary equation for each internal state variable contains two terms: one for hardening, and the other for recovery (either thermal or dynamic, but not both). This set of evolutionary equations is unique to this work. A prime objective in the development of this thermoviscoplastic model was to make the model as simple as the physics and intended applications allow. The fact that thermal and dynamic recovery terms are not coupled in any of the evolutionary equations is such a simplification. As a result, the material functions for the model are constructed readily using established phenomenological relationships. The use of both isotropic and kinematic variables is necessary to accurately model the anisothermal, cyclic, multiaxial, loading states found in power system applications. It might be possible to accurately model other applications, such as metal forming (ref. 21), by using only one internal state variable.

A wide range of materials are used in devices that are designed to operate in high-temperature environments. The designer's choice of material is often dictated by its ability to carry load at high temperatures, or to conduct heat. Whenever a design calls for a material of high conductivity, copper is often the material of choice. For example, a copper-based alloy (NARloy-Z) is used as a liner in the regeneratively cooled combustion chamber of the space shuttle main engines.

This report describes a thermoviscoplastic model for copper with this type of application in mind. As an aid to the reader, a list of symbols is provided in the appendix.

Constitutive Assumptions

We shall consider the anisothermal behavior of viscoplastic materials, such as polycrystalline metals. Each element of the material is assumed to be isotropic and to carry no stress in its initial virgin condition. However, as the material deforms, it may lose all or some of its symmetries. Small strains, displacements, and rotations make up the deformation of the material. Strain ϵ is decomposed into elastic ϵ^e (reversible) and inelastic, or plastic, ϵ^p (irreversible) contributions

$$\epsilon = \epsilon^e + \epsilon^p \tag{1}$$

with no net elastic or inelastic strains occurring in the stress-free virgin condition.

The changing internal structure of a material element is characterized by its state (σ, α_i, T). Stress σ is the measure of elastic change in internal structure, while the internal state variables α_i (for $i = 1, 2, \ldots, m$) are the measures of inelastic change in internal structure. This inelastic change affects the future response of the material element. Temperature T may also influence the elastic and inelastic aspects of internal structure.

Consider those materials whose behavior under thermomechanical loading conditions accepts the following general constitutive representation

$$tr(\epsilon) = \frac{1 - 2\nu}{E} tr(\sigma) + 3\alpha \Delta T \tag{2}$$

$$\boldsymbol{e} = \frac{1 + \nu}{E} \boldsymbol{S} + \epsilon^p \tag{3}$$

and

$$A_i = \sum_{j=1}^{m} H_{ij}\alpha_j \tag{4}$$

where

$$\dot{\epsilon}^p = \dot{\epsilon}^p(\sigma, \alpha_j, T) \tag{5}$$

and

$$\dot{\alpha}_i = \dot{\alpha}_i(\sigma, \alpha_j, T) \tag{6}$$

such that $\dot{\epsilon}^p$ and $\dot{\alpha}_i$ both vanish in the stress-free virgin state. (A dot placed over a variable denotes its time rate of change.) The deviatoric stress $\boldsymbol{S}$ and deviatoric strain $\boldsymbol{e}$ are defined by

$$\boldsymbol{S} = \boldsymbol{\sigma} - \frac{1}{3} tr(\boldsymbol{\sigma})\boldsymbol{I} \tag{7}$$

and

$$\boldsymbol{e} = \boldsymbol{\epsilon} - \frac{1}{3} tr(\boldsymbol{\epsilon})\boldsymbol{I} \tag{8}$$

where $\boldsymbol{I}$ is the unit tensor. The elastic response is governed by linear isotropic thermoelasticity, where E, α, and ν are the material constants. The inelastic response is considered incompressible causing the inelastic strain to be deviatoric. Onsager relations (ref. 26) are used to relate the internal state variables (or fluxes) α_i to their conjugate thermodynamic forces (or affinities) A_i through a symmetric nonnegative matrix of moduli H_{ij}, which typically vary with temperature. (The coefficient of thermal expansion α is not to be confused with the internal state variables α_i.)

The inelastic strain and the internal state variables both evolve as functions of state. Since stress rate and temperature rate are not state variables, equation (6) implies that sudden changes in stress and/or temperature do not alter the internal structure of the material. Such constant structure experiments provide useful information about the stress and temperature dependence of inelastic strain rate.

Theories of plasticity, creep, and viscoplasticity typically use state spaces that incorporate the thermodynamic forces A_i instead of their conjugate fluxes α_i. This is accomplished by using equation (4) to rewrite equations (5) and (6) as

$$\dot{\epsilon}^p = \dot{\epsilon}^p(\sigma, A_j, T) \tag{9}$$

and

$$\dot{\alpha}_i = \dot{\alpha}_i(\sigma, A_j, T) \tag{10}$$

and therefore, in accordance with equation (4),

$$\dot{A}_i = \sum_{j=1}^{m} H_{ij}\dot{\alpha}_j + \sum_{j,k=1}^{m} \frac{\partial H_{ij}}{\partial T} H_{jk}^{-1} A_k \dot{T} \tag{11}$$

establishes the evolutionary form for the thermodynamic forces, independent of the thermodynamic fluxes. The last term in this equation accounts for the temperature dependence of the Onsager moduli, which can be important in practical applications with variable temperature histories.

This constitutive theory must satisfy the thermodynamic constraint of intrinsic material dissipativity (refs. 27 and 28) defined by

$$\sigma : \dot{\epsilon}^p \geq \sum_{i=1}^{m} A_i \dot{\alpha}_i \tag{12}$$

which is a consequence of the laws of thermodynamics.[1] This constraint states that the rate of inelastic work done on a material element must equal or exceed the rate of increase in energy stored by the material due to a changing internal structure. (The notation : signifies a double tensorial contraction.)

A special class of materials (called Ω-form (refs. 28 and 29), or standard (ref. 27), materials) satisfies dissipativity by defining a positive scalar-valued function

$$\Omega = \Omega(\sigma, A_j; T) \tag{13}$$

that vanishes only in the stress-free virgin state. The rate effects of the theory (eqs. (9) and (10)) are then assumed to be governed by the generalized normality relationships

$$\dot{\epsilon}^p = \frac{\partial \Omega}{\partial \sigma} \tag{14}$$

and

$$\dot{\alpha}_i = -\frac{\partial \Omega}{\partial A_i} \tag{15}$$

which necessarily satisfy dissipativity if the set of all possible surfaces $\{\Omega = \text{constant}\}$ is composed of elements that are convex, that are nested, and that contain the origin ($\sigma = A_i = 0$). There are many models in the published literature that support an Ω-form (e.g., refs. 9, 12, and 30). It is not necessary, however, that all models represent Ω-form materials, since Ω-form materials are but a subset of the set of all thermodynamically admissible viscoplastic models. An example of a model that does not admit an Ω-form is presented in this report.

Thermoviscoplastic Model

The thermoviscoplastic model presented herein uses three internal state variables: they are a deviatoric tensor $\boldsymbol{\beta}$ and two positive-valued scalars δ and λ. Their conjugate forces are referred to as the (deviatoric) back stress $\boldsymbol{B}$, the drag stress D, and the limit stress L, respectively. The back stress accounts for kinematic hardening effects, while the drag and limit stresses account for isotropic hardening effects. To assure an initial condition that is isotropic, $\boldsymbol{\beta}(0) = 0$. As $\boldsymbol{\beta}$ evolves, the material develops a flow-induced anisotropy.

A simplified structure for a viscoplastic model is proposed in that there is no coupling between separate thermal and dynamic recovery terms in any of the evolutionary equations. This facilitates the derivation of material functions presented in the next section. The proposed thermoviscoplastic model is characterized by the flow equation

$$\dot{\epsilon}^p = \Theta Z(F) \frac{\boldsymbol{\Sigma}}{\Sigma_2} \tag{16}$$

and by the evolutionary equations for the thermodynamic fluxes

$$\dot{\boldsymbol{\beta}} = \dot{\epsilon}^p - \frac{\mathbf{B}}{L} \dot{\epsilon}_2^p \tag{17}$$

$$\dot{\delta} = \frac{1}{G}\left[\dot{\epsilon}_2^p - \Theta R(G)\right] = \frac{1}{G}\left[1 - \frac{R(G)}{Z(F)}\right]\dot{\epsilon}_2^p \tag{18}$$

and

$$\dot{\lambda} = \frac{D}{L}[F - G]\dot{\epsilon}_2^p = \left[\frac{\Sigma_2}{L} - \frac{D}{C - D}\right]\dot{\epsilon}_2^p \tag{19}$$

or, equivalently, by the evolutionary equations for the thermodynamic forces (see eq. (11))

$$\dot{\boldsymbol{B}} = H_b\left[\dot{\epsilon}^p - \frac{\boldsymbol{B}}{L}\dot{\epsilon}_2^p\right] + \frac{\boldsymbol{B}}{H_b}\frac{\partial H_b}{\partial T}\dot{T} \tag{20}$$

$$\dot{D} = \frac{H_d}{G}\left[\dot{\epsilon}_2^p - \Theta R(G)\right] + \frac{D}{H_d}\frac{\partial H_d}{\partial T}\dot{T} \tag{21}$$

and

$$\dot{L} = \frac{H_\ell D}{L}[F - G]\dot{\epsilon}_2^p + \frac{L}{H_\ell}\frac{\partial H_\ell}{\partial T}\dot{T} \tag{22}$$

where

$$F = \frac{\Sigma_2}{D} \tag{23}$$

[1]Thermal and intrinsic dissipation are not coupled, since equations (9) and (10) define the state space as being independent of the thermal gradient (see ref. 27).

$$G = \frac{L}{C - D} \tag{24}$$

$$\boldsymbol{\Sigma} = \boldsymbol{S} - \boldsymbol{B} \tag{25}$$

$$\Sigma_2 = \sqrt{\frac{1}{2}\,\boldsymbol{\Sigma} : \boldsymbol{\Sigma}} \tag{26}$$

and

$$\dot{\epsilon}_2^p = \sqrt{\frac{1}{2}\,\dot{\boldsymbol{\epsilon}}^p : \dot{\boldsymbol{\epsilon}}^p} \tag{27}$$

Here C, H_b, H_d, and H_ℓ are positive-valued material constants, $\Theta > 0$ is the thermal diffusivity, $Z = \dot{\epsilon}_2^p/\Theta \geq 0$ is the Zener-Hollomon (ref. 31) parameter, $R \geq 0$ is the thermal recovery function, $F \geq 0$ and $G \geq 0$ are flow functions, $\boldsymbol{\Sigma}$ is the effective stress associated with plastic flow, and Σ_2 and $\dot{\epsilon}_2^p$ are the magnitudes of effective stress and inelastic strain rate.

The flow equation, equation (16), is a second invariant formulation derived from a potential function (eq. (14), see ref. 29) in accordance with the thermodynamic development of Rice (ref. 32). First and third invariants are not introduced into the model because they result in higher order effects that are neglected in accordance with von Mises (ref. 33). This flow equation is compatible with the kinematic constructs proposed by Prager (ref. 34) in his theory of plasticity.

The isothermal form of the evolutionary equation for back stress, equation (20), was proposed by Armstrong and Frederick (ref. 35) for plasticity. Its anisothermal counterpart was subsequently used by Chaboche (ref. 10) and Walker (ref. 15) in their viscoplastic models. This evolutionary equation introduces an evanescent strain memory effect (evanescent along the plastic strain path) that is consistent with Il'yushin's hypothesis (delay-trace hypothesis (ref. 36)) that a material response depends not on the whole of the previous strain path, but only on the most recent part of it. In this evolutionary equation, strain-induced dynamic recovery competes against strain hardening. This competitive process causes the back stress $\boldsymbol{B}$ to evolve exponentially to an asymptotic limit stress L associated with kinematic saturation $B_{2\text{sat}}$. A graphic illustration of this evanescent concept is given in figure 1. Here the limiting state of back stress defines a hypersurface of radius L in state space. Whenever this upper bound is reached, a perfectly plastic or creeplike response is attained, provided that the material has also isotropically saturated. At kinematic saturation, the inelastic strain rate $\dot{\boldsymbol{\epsilon}}^p$ becomes coaxial with both the deviatoric stress $\boldsymbol{S}$ and the back stress $\boldsymbol{B}$ (in agreement with the experimental observations of Phillips (ref. 37)), and the nested set of flow surfaces $\{\Sigma_2 = \text{constant}\}$ becomes stationary until unloading occurs. Otherwise, this set of flow

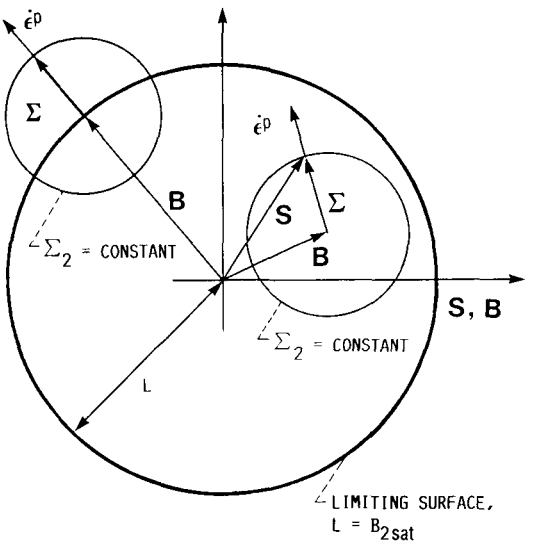

Figure 1.—State space representation of limiting state of back stress.

surfaces can translate freely within the limiting surface, as governed by the flow and evolutionary equations.

The evolutionary equation for drag stress, equation (21), is consistent with the Bailey-Orowan (refs. 38 and 39) hypothesis of thermally induced recovery competing against strain hardening. It has been used by the author (ref. 40) in its isothermal form. Inclusion of the temperature dependence of the hardening (Onsager) modulus H_d has not appeared in previous viscoplastic models. This evolutionary equation has the drag stress harden at the rate $H_d\dot{\epsilon}_2^p/G$, which equals $H_d(C - D)\dot{\epsilon}_2^p/L$ because of equation (24). Therefore, similar to the back stress, the drag stress hardens exponentially to an asymptotic limit C. This evolutionary equation for drag stress therefore has the concept of dynamic recovery built into the equation without introducing a separate term for it. However, unlike the back stress, the effect of strain hardening can never be completely cancelled out by the influence of dynamic recovery at the isotropic saturation of state; the influence of thermal recovery is also required because $C > D$ for all values of drag stress. Notice also that this expression for thermal recovery can be cast into a strain-induced dynamic recovery format, as witnessed in equation (18).

The evolutionary equation for limit stress, equation (22), is unique to this work. The concept of the limit stress evolving as a state variable is not a new idea (as it has been used by Marquis (ref. 41) and Walker (ref. 15)), but rather, it is the form of the equation that is new. In the models of Marquis and Walker, the limit stress evolves exponentially by a relationship of the form

$$\dot{L} = H_\ell \left[1 - \frac{L}{L_{\text{sat}}} \right] \dot{\epsilon}_2^p \tag{28}$$

to an asymptotic saturation value of the limit stress L_{sat}.

Actually, both authors chose to express the limit stress as a function of accumulated inelastic strain by integrating equation (28), thereby eliminating the need of explicitly defining the limit stress as a state variable. In the model proposed herein, the term in the bracket of equation (28) is replaced by a difference between the two flow functions, (i.e., $D(F - G)/L$), a result derived from thermodynamic and steady-state considerations. The thermodynamic constraint of dissipativity, which motivated the choice of D/L as the coefficient to the difference $(F - G)$, is discussed in the next paragraph. At steady state, the flow function F is related to the magnitude of deviatoric stress

$$S_2 = \sqrt{\frac{1}{2}\, \boldsymbol{S} : \boldsymbol{S}} \tag{29}$$

by definition through the relation

$$F\,|_{ss} = \frac{S_2}{C} \tag{30}$$

where ss denotes steady state. The flow function F simplifies to

$$F\,|_{ss} = \left.\frac{\Sigma_2}{D}\right|_{ss} = \left.\frac{S_2 - B_2}{D}\right|_{ss} = \left.\frac{S_2 - L}{D}\right|_{ss} \tag{31}$$

at steady state, which when combined with equation (30) enables one to determine another flow function: that is,

$$G|_{ss} = \left.\frac{L}{C - D}\right|_{ss} = \frac{S_2}{C} \tag{32}$$

where

$$B_2 = \sqrt{\frac{1}{2}\, \boldsymbol{B} : \boldsymbol{B}} \tag{33}$$

is the magnitude of back stress. The flow functions F and G are defined to be equal at steady state—a result that must be true if equations (19) and (22) are to have meaning (since $\dot{\boldsymbol{\beta}} = \dot{\delta} = \dot{\lambda} = 0$ at steady state, by definition). The derivation of equation (31) makes use of the facts that $\Sigma_2 = (S_2 - B_2)$ and $B_2 = L$ at steady state (neither of which is true, in general, under other conditions). Looking at equation (32), one can ask: Which state variable (L, D, or both) accounts for the stress dependence S_2 at steady state? To answer this question, a nonlinear, least-squares, optimization algorithm (ref. 42) was used to determine the saturated values L_{sat} and D_{sat} from stable hysteresis loops of stress versus strain, where kinematic saturation occurred prior to each reversal. Several experiments with a range of 6 to 1 in stress amplitude (obtained at different temperatures) were used. The result was the saturated value of limit stress L_{sat} varied with applied stress, whereas, the saturated value of drag stress D_{sat} was independent of applied stress. The proposed evolutionary equation for limit stress, equation (22), is consistent with this observation (the stress dependence enters through the flow function F, as evident in eq. (19)). Plus, it provides a self-consistency to the model in that its flow and evolutionary equations reduce to the multiaxial formulation

$$\dot{\boldsymbol{\epsilon}}^p\big|_{ss} = \Theta\, Z\left(\frac{S_2}{C}\right)\frac{\boldsymbol{S}}{S_2} \tag{34}$$

at steady state, which is the flow equation used in the classical theory of creep (ref. 43).

For this viscoplastic model to be thermodynamically admissible, it must satisfy the constraint of dissipativity given in equation (12), which becomes

$$\boldsymbol{\sigma} : \dot{\boldsymbol{\epsilon}}^p \geq \boldsymbol{B} : \dot{\boldsymbol{\beta}} + D\dot{\delta} + L\dot{\lambda} \tag{35}$$

Combining this inequality with the constitutive equations given in equations (16) to (19) results in the constraint

$$R \geq Z\left[1 - G\left(F + G + 2\,\frac{B_2^2}{LD}\right)\right] \tag{36}$$

which bounds thermal recovery from below. This constraint will seldom, if ever, be realized in any given analysis, but nevertheless, it is a physically mandatory constraint.[2] All the parameters in this inequality are nonnegative valued by definition; therefore, this inequality is satisfied whenever the inner bracketed term exceeds 1 in value, which is typically the case. Dissipativity provides a real constraint when choosing forms for evolutionary equations. In particular, the hardening terms are the ones that cause constraint; whereas, the recovery terms are of a thermodynamic benefit. For example, if the term $D(F - G)/\mathrm{L}$ found in the evolutionary equation for limit stress, equation (22), was replaced by the difference $(F - G)$, then the constraint of dissipativity would require that

$$R \geq Z\left[1 - FG\left(\frac{L}{D} - 1\right) - G\left(F + G + 2\,\frac{B_2^2}{LD}\right)\right] \tag{37}$$

[2]In the numerical computations done for this report, this thermoviscoplastic model satisfied dissipativity at all states except at the very onset of deformation, (i.e., at the initial condition). Whenever the inequality of equation (36) was not satisfied, the thermal recovery function R was set equal to the right-hand side of equation (36), thereby satisfying thermodynamics.

instead of equation (36). The additional term $FG[(L/D) - 1]$ is sufficient to cause this inequality to not be satisfied in practice (at least that was the author's experience).

In addition to the constraint of dissipativity given in equation (36), thermal recovery R is also constrained by the fact that the internal state variable δ associated with the drag stress D cannot dip below a minimum value δ_0 associated with the virgin, or annealed, state.

The constitutive equation for the evolution of back stress is isotropic, as presented in equation (20), since a scalar H_b replaces the general, nonnegative, fourth-order tensor $\boldsymbol{H}_b$ for the hardening modulus.[3] For anisotropic materials, the back stress evolves as

$$\dot{\boldsymbol{B}} = \boldsymbol{H}_b : \left(\dot{\boldsymbol{\epsilon}}^p - \frac{\boldsymbol{B}}{L} \dot{\epsilon}_2^p \right) + \frac{\partial \boldsymbol{H}_b}{\partial T} : \left(\boldsymbol{H}_b^{-1} : \boldsymbol{B} \right) \dot{T} \tag{38}$$

and in accordance with Lee and Zaverl (ref. 44), the flow equation becomes

$$\dot{\boldsymbol{\epsilon}}^p = \Theta Z(F) \frac{\boldsymbol{M} : \boldsymbol{\Sigma}}{\sqrt{\frac{1}{2} \boldsymbol{\Sigma} : \boldsymbol{M} : \boldsymbol{\Sigma}}} \tag{39}$$

where

$$F = \frac{\sqrt{\frac{1}{2} \boldsymbol{\Sigma} : \boldsymbol{M} : \boldsymbol{\Sigma}}}{D} \tag{40}$$

and $\boldsymbol{M}$ is a nonnegative fourth-order tensor that is a measure of anisotropy. The actual characterizations of $\boldsymbol{H}_b$ and $\boldsymbol{M}$ are beyond the scope of this paper. Nevertheless, as a first approximation it may be reasonable to consider

$$\boldsymbol{H}_b = H_b \boldsymbol{M} \tag{41}$$

so that the strength of anisotropy is the same for both tensors. The fact that the hardening (Onsager) modulus for the back stress is, in general, a fourth-order tensor seems to have eluded viscoplastic modelers.

Material Functions

Before the thermoviscoplastic model of the previous section can be used to model a material or a class of materials, specific forms for its material functions Θ, R, and Z must be determined. Physically based phenomenological relations are used to meet this need. Conditions of steady-state flow provide the form of these functions for the class of materials considered (i.e., polycrystalline metals and Class II solid solution alloys where solute drag effects are negligible (refs. 8, 16, and 20)).

The temperature dependence of the model is largely contained within the thermal diffusivity parameter, which is taken to be (ref. 45)

$$\Theta = \begin{cases} \exp\left(\dfrac{-Q}{kT}\right) & \text{for} \quad T \geq \dfrac{T_m}{2} \\ \exp\left\{\dfrac{-2Q}{kT_m}\left[\ln\left(\dfrac{T_m}{2T}\right) + 1\right]\right\} & \text{for} \quad T \leq \dfrac{T_m}{2} \end{cases} \tag{42}$$

where Q is the activation energy for self-diffusion, T_m is the absolute melting temperature, and kT has its usual meaning. This relationship represents an apparent activation energy, as depicted in figure 2 for creep of copper. The cluster of datum points that falls below the main trend of the data (in the range of about 0.5 to 0.6 homologous temperature) is attributed to dislocation enhanced diffusion (ref. 46). The author's attempt to account for this additional mechanism resulted in a poorer correlation of the Zener-Hollomon parameter than that which is presented in figure 3.

Since the steady-state flow of metals can be modeled by a power law at the lower stresses and an exponential at the higher stresses (ref. 47), one can write the steady-state Zener-Hollomon parameter associated with equation (34) as (ref. 40)

$$Z\left(\frac{S_2}{C}\right) = \frac{\dot{\epsilon}_2^p}{\Theta} = \begin{cases} A\left(\dfrac{S_2}{C}\right)^n & \text{for} \quad S_2 \leq C \\ A \exp\left[n\left(\dfrac{S_2 - C}{C}\right)\right] & \text{for} \quad S_2 \geq C \end{cases} \tag{43}$$

where A, C, and n are material constants. (The constant A is not to be confused with the thermodynamic forces A_i.) A plot of this parameter is presented in figure 3 for copper. This Zener-Hollomon parameter is defined so that it is continuous and differentiable across the interface $S_2 = C$ (i.e., the power-law breakdown stress), and is therefore equivalent to the hyperbolic function proposed by Garofalo (ref. 48). According to Nix and Gibeling (ref. 49), diffusional recovery mechanisms control the creep response in the low-stress, high-temperature, power-law domain; whereas, dynamic recovery

[3]Unlike classical elasticity which requires two scalars (e.g., E and ν) to represent the fourth-order elastic modulus in the isotropic case, the hardening modulus $\boldsymbol{H}_b$ requires only one (i.e., H_b) because the back stress is deviatoric.

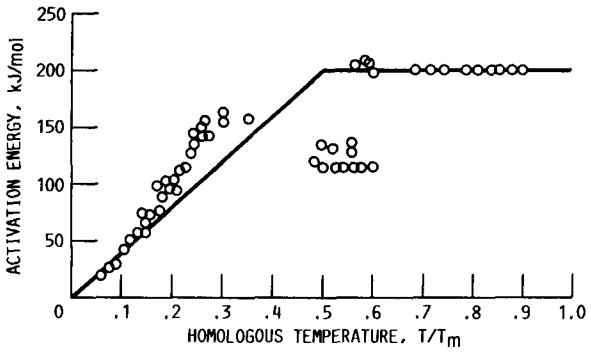

Figure 2.—Apparent activation energies for creep of copper. Data are as presented in reference 46. Solid line represents equation (42) for constants in table I.

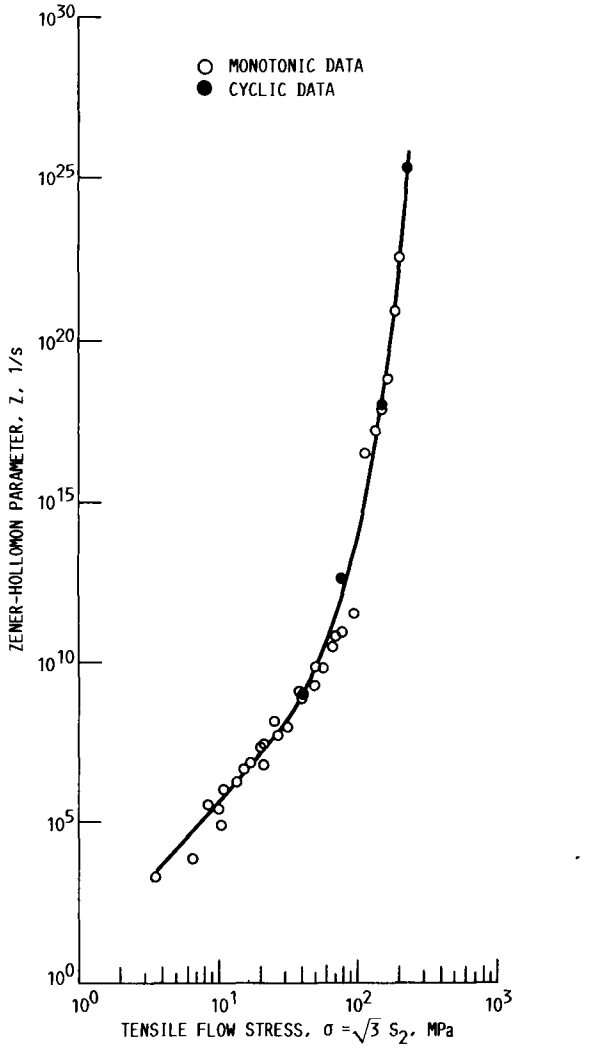

Figure 3.—Stress dependence of Zener-Hollomon parameter for copper. Data are as presented in reference 40. Curve represents fit of equation (43) to data for constants in table I.

mechanisms control the creep response in the high-stress, low-temperature, exponential (power-law breakdown) domain. In more conventional terms, creep is synonymous with a power-law response; whereas, limit plasticity is synonymous with an exponential response, where the flow stress appears to be strain-rate insensitive over a fairly large range in strain rate.

One can combine equations (30) and (43) to obtain the Zener-Hollomon parameter associated with equation (16); that is,

$$Z(F) = \begin{cases} AF^n & \text{for} \quad F \le 1 \\ A \exp[n(F-1)] & \text{for} \quad F \ge 1 \end{cases} \tag{44}$$

Likewise, noting that $F = G$ and $R = Z$ at steady state (a consequence of eqs. (18) and (19)), one obtains the thermal recovery function associated with equation (18): that is,

$$R(G) = \begin{cases} AG^n & \text{for} \quad G \le 1 \\ A \exp[n(G-1)] & \text{for} \quad G \ge 1 \end{cases} \tag{45}$$

Thus in accordance with Nix and Gibeling, recovery is controlled by diffusional mechanisms whenever $G < 1$, and by dynamic mechanisms whenever $G > 1$. This thermal recovery function is thermodynamically constrained by equation (36). It is also constrained to be zero valued in the virgin, or annealed, state where $\delta = \delta_o$ (if thermodynamically admissible). Since the flow functions F and G are not restricted to be steady-state parameters, the material functions given in equations (44) and (45) for the Zener-Hollomon parameter Z and the thermal recovery function R are assumed to be applicable to transient and steady-state conditions alike.

The thermoviscoplastic model has three elastic constants to determine:

$$E, \ \alpha, \text{ and } \nu$$

all of which can vary with temperature, and it has ten inelastic constants to determine:

$$A, \ C, \ \delta_o, \ H_b, \ H_d, \ H_\ell, \ \lambda_o, \ n, \ Q, \text{ and } T_m$$

of which only the three hardening (Onsager) moduli H_b, H_d, and H_ℓ can vary with temperature. Two material constants are required to characterize thermal diffusivity—Q and T_m, three to characterize steady state—A, C, and n, three to characterize transient behavior—H_b, H_d, and H_ℓ, and two to characterize the initial condition—δ_o and λ_o. The values of these elastic and inelastic constants are given in table I for copper.

TABLE I.—MATERIAL CONSTANTS FOR COPPER

Elastic constants[a]	
E, MPa	$127\,000 - 41T - 0.027T^2$
α, 1/°C	$16\text{x}10^{-6} + 5\text{x}10^{-9}T$
ν	0.34
Inelastic constants[a]	
A, 1/s	50 000 000
C, MPa	14.3
δ_o	0.0027
H_b, MPa	$50\,000 - 40T$
H_d, MPa	370
H_f, MPa	450
λ_o	0.027
n	5
Q, J/mol	200 000
T_m, K	1356

[a]Temperature T is in degrees centigrade; k = 8.314 J/mol K.

The activation energy for self-diffusion Q and the melting temperature T_m are handbook data.

With the thermal diffusivity now characterized, one can determine the Zener-Hollomon parameter $Z = \dot{\epsilon}_2^p/\Theta$ at steady state and plot it against its associated flow stress, as in figure 3. Each monotonic datum point in this figure represents the average of typically four to six creep experiments, usually run at different temperatures but with the same flow stress. The saturated, fully reversed, cyclic data are in agreement with the monotonic creep data. Values for the steady-state material constants A, C, and n are obtained by fitting these data to equation (43). They are quickly obtained by trial and error. The coefficient A translates the curve along the ordinate. The power-law breakdown stress C splits the stress domain into power-law and exponential stress-dependent domains. The exponent n defines the slope of the curve in the power-law domain.

With the thermal-diffusivity and steady-state material constants specified, one can determine the kinematic hardening modulus H_b from stable, stress-strain hysteresis loops where the isotropic state variables have saturated. To accomplish this, a nonlinear, least-squares optimization algorithm (ref. 42) was used to fit H_b and the saturated value D_{sat} to data obtained from stable hysteresis loops at 22, 200, 400, and 600 °C. Although it is not necessary to use such a technique, it is useful and expedient to do so. The experimental and correlated hysteresis loops are compared in figure 4. The degree of correlation is quite good.

Four material constants remain to be determined; they are the two isotropic hardening moduli H_d and H_f, and the two initial conditions for the isotropic state variables δ_o and λ_o. Once again, a nonlinear, least-squares optimization algorithm was used to determine numeric values for material constants. This was not necessary, but to determine these constants by trial and error would have been a tedious and time-consuming chore. Cyclic stress-strain data obtained from the virgin state to the cyclically stabilized state at 22, 200, 400, and 600 °C

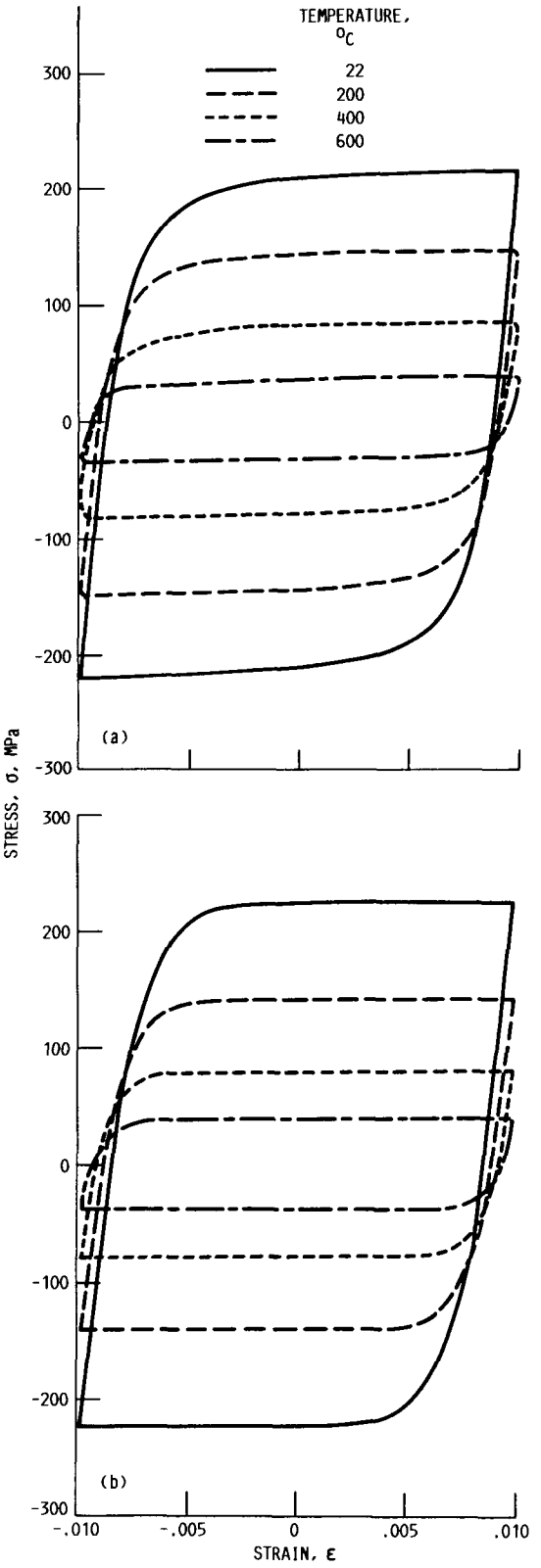

(a) Experimental data (ref. 40).
(b) Theoretical correlations.

Figure 4.—Saturated, uniaxial, hysteresis loops for copper. Strain rate, $\dot{\epsilon}$, 0.001/s.

were used for correlation purposes. An example of experimental and correlated stress-strain cycles is shown in figure 5. The degree of correlation is quite good.

The curve depicting the evolution of back stress in figure 5 provides useful insight into how the three internal state variables of this model interact with one another. The back stress provides the curvature in the stress-strain response. The cyclic hardening characteristic of the back stress is the consequence of an evolving limit stress. A small value of limit stress enables only a small amount of back stress at kinematic saturation. This results in a stress-strain response with sharper curvature, as observed in the initial, monotonic loading curve. The extent of separation between the applied stress and the back stress (i.e., the magnitude of effective stress) is a measure of strength associated with the drag stress. The increasing separation between these stresses with deformation is the consequence of an evolving drag stress.

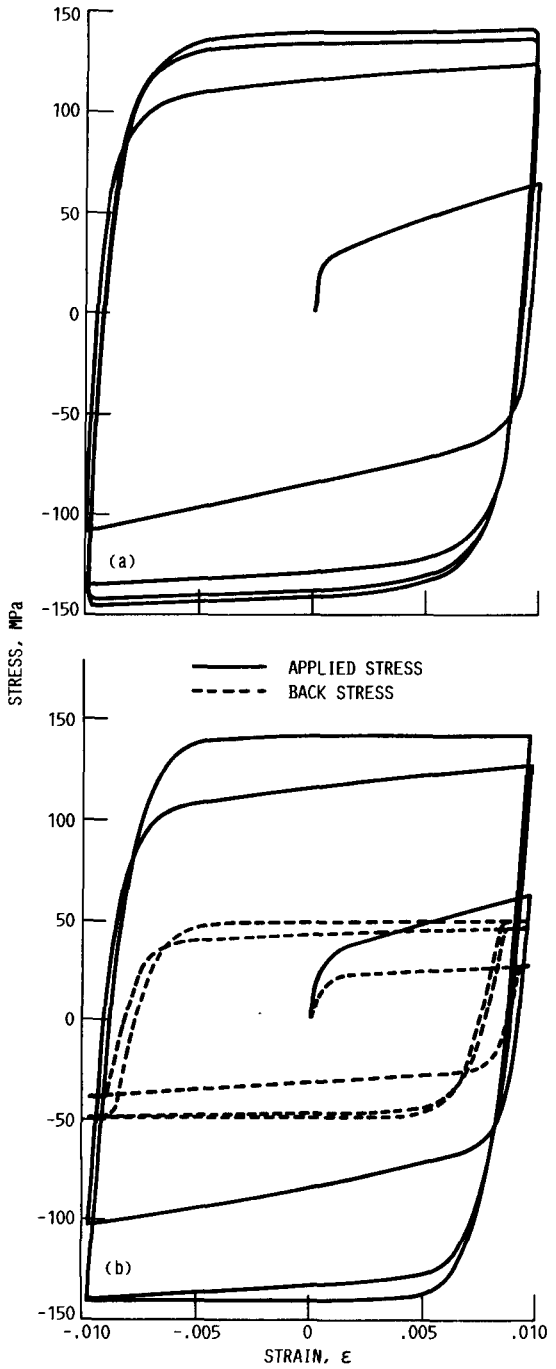

(a) Experimental data (ref. 40).
(b) Theoretical correlation.

Figure 5.—Uniaxial, cyclic, stress-strain response for copper. Temperature, T, 200 °C; strain rate, $\dot{\epsilon}$, 0.001/s.

Applications

Theoretical correlations are presented in the previous section; theoretical predictions are presented in this section. In particular, theoretical predictions are presented for thermomechanical and biaxial nonproportional tests for which experimental data exist in the literature.

A comparison between experiment and theory is presented in figure 6 for an inphase thermomechanical test of copper. The model's prediction is satisfactory. It does well at the tips of the loop, but not as well in the region of the Bauschinger effect. An earlier attempt to predict this experiment by the author (ref. 40) was less than satisfactory, because that model overpredicted the cold end response by some 50 percent. The difference is that in this model the limit stress evolves as a state variable, whereas in the previous model the limit stress varied only with temperature. Predictions were made with this model that both included and excluded the anisothermal $\dot{T}$ term in the evolutionary equations (eqs. (20) to (22)). For this particular application, the influence of this term on the predicted stress-strain response was negligible.

The experimental stress-strain curve presented in figure 6 has been smoothed. In reality (see ref. 40), strain avalanches occurred periodically along the response curve; a phenomenon that seems to accompany slower strain-rate experiments ($\dot{\epsilon} \lesssim 1\text{x}10^{-5}$/s) done on copper. Curiously, these strain avalanches were nonrandom events. After cyclic saturation was attained, they would repeat themselves in number, degree, and location along the response curve from cycle to cycle. No attempt is made by continuum viscoplasticity to model strain avalanching.

Experimental data from a cyclic, nonproportional, axial-torsional test done on an isotropically saturated copper specimen by Lamba and Sidebottom (ref. 50) are presented in figure 7. Theoretical predictions of this experiment are presented in figure 8 for three different models. One is the thermoviscoplastic model developed herein. The other two are plasticity models considered by Lamba and Sidebottom. In particular, they are a Krieg-Dafalias (refs. 51 and 52) two-surface plasticity model with a Tresca yield condition, and a Prager (ref. 34) plasticity model with a von Mises yield

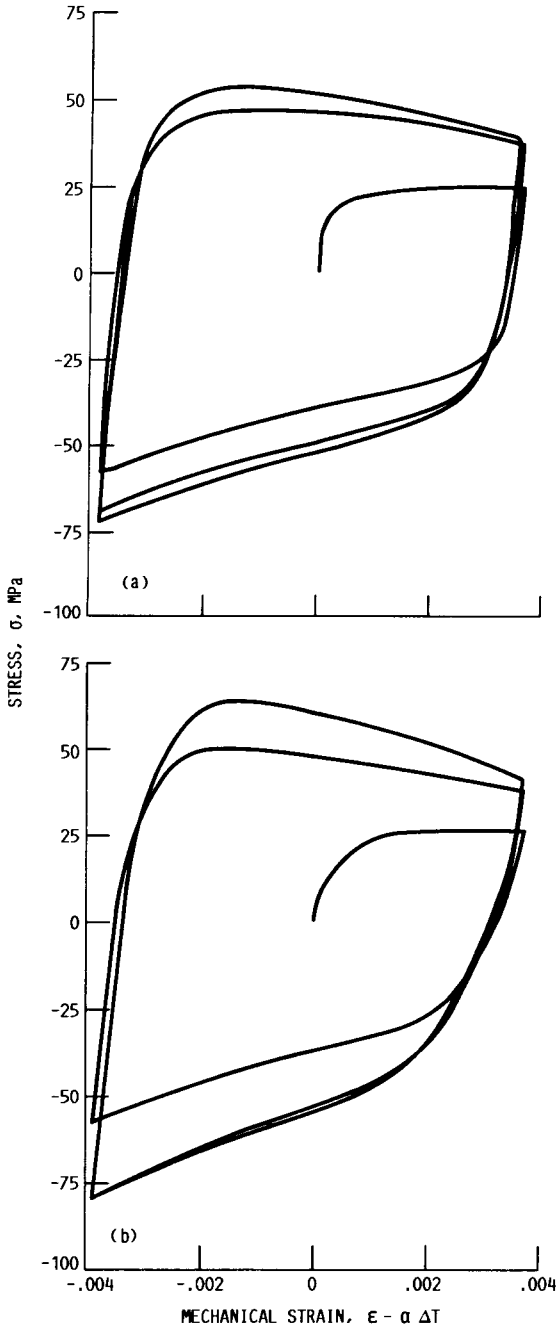

(a) Experimental data (ref. 40).
(b) Theoretical prediction.

Figure 6.—Uniaxial, inphase, thermomechanical, stress-strain response for copper. Temperature, T, 200 to 500 °C; temperature rate, $\dot{T}$, constant; strain rate, $\dot{\epsilon}$, $1.5 \times 10^{-5} + \alpha\dot{T}$/s.

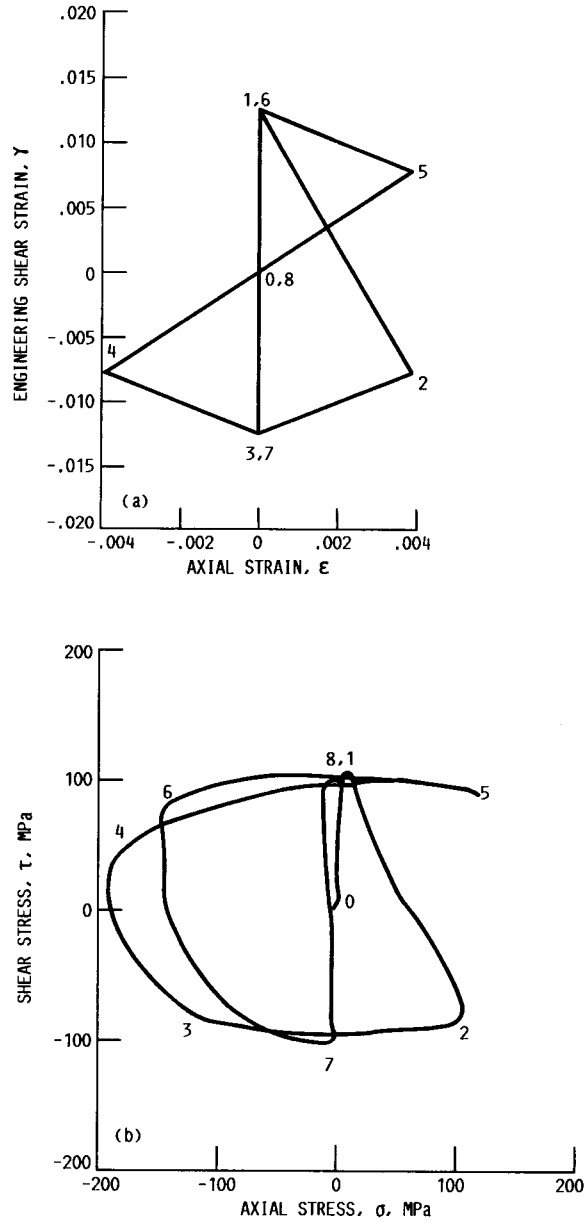

(a) Strain control program.
(b) Experimental stress response.

Figure 7.—Cyclic, nonproportional, axial-torsional test of copper at room temperature. Test specimen cycled to isotropic saturation prior to testing. Path segments sequenced from 0 → 1 → 2 → ... → 8. Each path segment applied in 60 s. Data are as presented in reference 50.

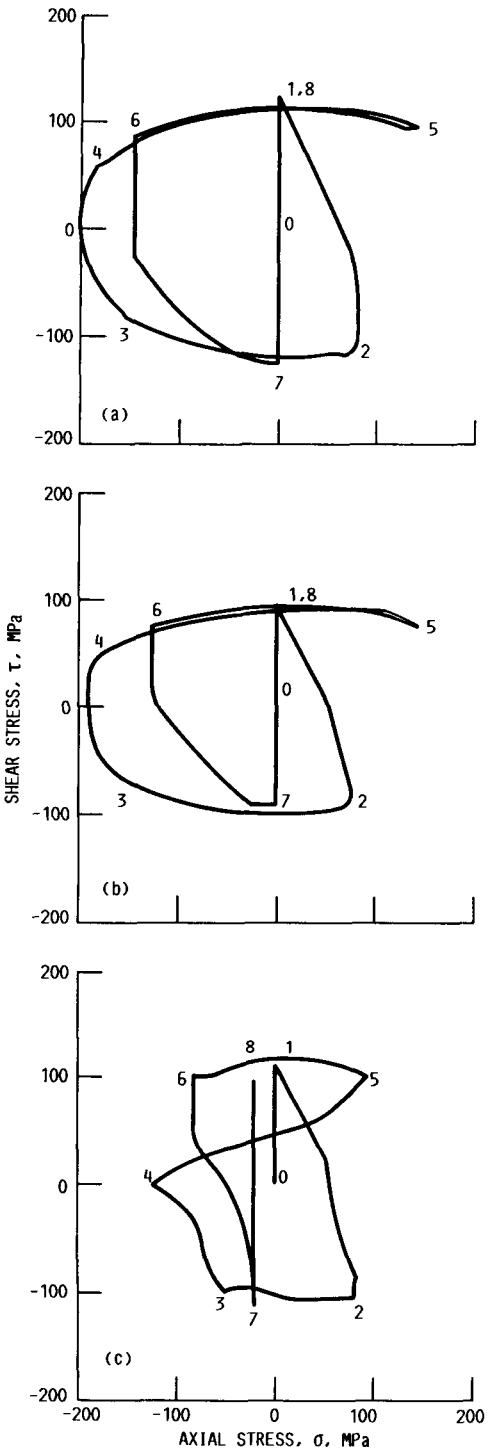

(a) Thermoviscoplastic model.

(b) Krieg-Dafalias, two-surface, plasticity model. Data are as presented in reference 50.

(c) Prager plasticity model. Data are as presented in reference 50.

Figure 8.—Theoretical predictions of three models for the cyclic, nonproportional, axial-torsional test of figure 7.

condition.[4] The viscoplastic model has a von Mises-like yield condition because it is a second invariant formulation. All three of these models were formulated such that they exhibit a strain hardening response that exponentially decays with continued directional deformation. Under proportional loading conditions, these three models produce nearly equivalent stress-strain responses (the difference being the rate dependence of the viscoplastic model versus the rate independence of the plasticity models).

The viscoplastic model and the Krieg-Dafalias model both do a good job of representing the experimental data. The Prager model, however, does poorly. In addition, the Prager model predicts a ratcheting response that was not observed experimentally. The other two models do not. The Prager model differs from the other two models in that it does not incorporate the concept of limit plasticity. In particular, it does not require the inelastic strain rate $\dot{\epsilon}^p$ to be coaxial with the deviatoric stress $\boldsymbol{S}$ and the back stress $\boldsymbol{B}$ at kinematic saturation. The Krieg-Dafalias model introduces the concept of limit plasticity through a second yield surface (after the manner of Mroz (ref. 54)) where the plastic modulus is zero valued; it is the limit surface. The viscoplastic model introduces the concept of limit plasticity through the evolutionary equation for back stress (eq. (20)) as illustrated in figure 1. Here the limit stress L represents the limiting state of back stress. Whenever the back stress attains this value, the response becomes one of perfect, or limit, plasticity, provided that the isotropic state variables have saturated, too. Lamba and Sidebottom (ref. 50) conclude by stating that "For a given path in strain space, the path in stress space is determined more by limit plasticity than by any other consideration." Therefore, viscoplastic models that do not embody the concept of limit plasticity (e.g., Bailey-Orowan formulations for the evolution of back stress) cannot properly model the plastic behavior of metals.

Comparing the viscoplastic and Krieg-Dafalias model predictions with the experimental data, one notices that the viscoplastic model does slightly better in predicting the axial response, while the Krieg-Dafalias model does slightly better in predicting the shear response. The reason why the Krieg-Dafalias model predicts shear better than the viscoplastic model has to do with the choice of yield and limit conditions. The Krieg-Dafalias model of Lamba and Sidebottom used Tresca yield and limit conditions, while the viscoplastic model uses von Mises-like yield and limit conditions. A better shear response could be predicted for these copper data if the third invariant were also considered in the formulation of the viscoplastic model. The approach of Robinson and Ellis (ref. 55) for incorporating the third invariant into a viscoplastic

[4]Lamba and Sidebottom (ref. 50) also considered a Ziegler (ref. 53) plasticity model with a Tresca yield condition. These results are not reproduced here because they are qualitatively equivalent to those obtained from the Prager model.

model is worthy of consideration. In contrast with the data of Lamba and Sidebottom (ref. 50), the copper data of Taylor and Quinney (ref. 56) support the von Mises yield condition over that of Tresca. One is therefore justified in considering the influence of the third invariant of stress on the inelastic flow of copper as a higher order effect.

Summary of Results

A primitive set of constitutive equations are considered from which a thermoviscoplastic model is developed. These equations assume that the material is initially isotropic, that the infinitesimal strain is additively decomposed into elastic and inelastic contributions, that the inelastic response is incompressible, that Onsager relations apply to the internal state variables, and that the inelastic strain and internal state variables evolve as functions of state. Associated with this set of constitutive equations is a thermodynamic constraint of intrinsic, or material, dissipativity that must always be satisfied.

A thermoviscoplastic model is developed that is a special case of this primitive set of constitutive equations. A second invariant formulation with three internal state variables is considered. One internal variable (the back stress) accounts for kinematic or flow-induced anisotropic effects, while the other two variables account for isotropic effects. Of the two isotropic variables, the drag stress is a measure of yield strength, while the limit stress is a measure of limit strength. Each evolutionary equation is composed of two terms; a hardening term and a recovery term (either dynamic or thermal, but not both). The fact that there is no coupling between dynamic and thermal recovery terms in any evolutionary equation is a simplification that enables the model to reduce to both plasticity and creep models in their respective limits.

There are three material functions in the model that must be characterized before it can be used for applications. They have been determined phenomenologically for copper. These functional forms should apply to the class of materials containing polycrystalline metals and Class II solid solution alloys where the effects of solute drag on strength are negligible.

A variety of model correlations and predictions are presented for copper under isothermal, thermomechanical, and nonproportional, cyclic conditions. All do a good job of describing the experimental data. One can therefore feel comfortable about using this model in real world structural design problems, such as regeneratively cooled combustion liners of rocket engines.

Lewis Research Center
National Aeronautics and Space Administration
Cleveland, Ohio, August 23, 1988

Appendix – Symbols

A coefficient for inelastic strain rate

A_i thermodynamic forces (or affinities)

$\boldsymbol{B}$ back stress (deviatoric)

C power-law breakdown stress

D drag stress

E Young modulus

$\boldsymbol{e}$ deviatoric strain

F,G flow functions

H_b hardening modulus for back stress

$\boldsymbol{H}_b$ nonnegative, fourth-order, anisotropic tensor for the hardening modulus for back stress

H_d hardening modulus for drag stress

H_{ij} Onsager hardening moduli

H_ℓ hardening modulus for limit stress

$\boldsymbol{I}$ unit tensor

k Boltsmann constant

L limit stress

$\boldsymbol{M}$ nonnegative, fourth-order, plastic, anisotropic tensor

n power-law creep exponent

Q activation energy for self-diffusion

R thermal recovery function

$\boldsymbol{S}$ deviatoric stress

T absolute temperature

T_m absolute melting temperature

Z Zener-Hollomon parameter

α coefficient of thermal expansion

α_i thermodynamic displacements (or fluxes)

$\boldsymbol{\beta}$ thermodynamic flux conjugate to back stress (deviatoric)

δ thermodynamic flux conjugate to drag stress

ϵ infinitesimal strain

Θ thermal diffusivity

λ thermodynamic flux conjugate to limit stress

ν Poisson ratio

$\boldsymbol{\sigma}$ Cauchy stress

$\boldsymbol{\Sigma}$ effective stress associated with plastic flow (deviatoric)

Ω potential function

Subscripts:

i,j,k indices

o value associated with initial or virgin states

sat saturated condition

ss steady state

2 magnitude of second-order tensor normalized for shear

Superscripts:

e elastic

p plastic (inelastic)

$\dot{}$ time rate of change

References

1. Saltsman, J.F.; and Halford, G.R.: Life Prediction of Thermomechanical Fatigue Using Total Strain Version of Strainrange Partitioning (SRP): A Proposal. NASA TP-2779, 1988.
2. Stowell, E.Z.: A Phenomenological Relation Between Stress, Strain Rate, and Temperature for Metals at Elevated Temperatures. NACA TN-4000, 1957.
3. Prager, W.: Linearization in Visco-Plasticity. Oesterr. Ing. Arch., vol. 15, no. 1-4, 1961, pp. 152-157.
4. Perzyna, P.: The Constitutive Equations for Rate Sensitive Plastic Materials. Q. Appl. Math., vol. 20, no. 4, Jan. 1963, pp. 321-332.
5. Geary, J.A.; and Onat, E.T.: Representation of Non-Linear Hereditary Mechanical Behavior. ORNL TM-4525, 1974.
6. Bodner, S.R.; and Partom, Y.: Constitutive Equations for Elastic-Viscoplastic Strain-Hardening Materials. J. Appl. Mech., vol. 42, no. 2, June 1975, pp. 385-389.
7. Hart, E.W.: Constitutive Relations for the Nonelastic Deformation of Metals. J. Eng. Mater. Technol., vol. 98, no. 3, July 1976, pp. 193-202.
8. Miller, A.: An Inelastic Constitutive Model for Monotonic, Cyclic, and Creep Deformation: Part 1—Equations Development and Analytical Procedures. J. Eng. Mater. Technol., vol. 98, no. 2, Apr. 1976, pp. 97-105.
9. Ponter, A.R.S.; and Leckie, F.A.: Constitutive Relationships for the Time-Dependent Deformation of Metals. J. Eng. Mater. Technol., vol. 98, no. 1, Jan. 1976, pp. 47-51.
10. Chaboche, J.L.: Viscoplastic Constitutive Equations for the Description of Cyclic and Anisotropic Behavior of Metals. Bull. Acad. Pol. Sci., Ser. Sci. Tech., vol. 25, no. 1, 1977, pp. 39-48.
11. Krieg, R.D.; Swearengen, J.C.; and Rohde, R.W.: A Physically-Based Internal Variable Model for Rate-Dependent Plasticity. Inelastic Behavior of Pressure Vessel and Piping Components, T.Y. Chang and E. Krempl, eds., ASME, 1978, pp. 15-28.
12. Robinson, D.N.: A Unified Creep-Plasticity Model for Structural Metals at High Temperature. ORNL TM-5969, 1978.
13. Stouffer, D.C.; and Bodner, S.R.: A Constitutive Model for the Deformation Induced Anisotropic Plastic Flow of Metals. Int. J. Eng. Sci., vol. 17, no. 6, 1979, pp. 757-764.
14. Valanis, K.C.: Fundamental Consequences of a New Intrinsic Time Measure. Arch. Mech. Stosow., vol. 32, no. 2, 1980, pp. 171-191.
15. Walker, K.P.: Research and Development Program for Nonlinear Structural Modeling with Advanced Time-Temperature Dependent Constitutive Relationships. (PWA-5700-50, United Technologies Research Center, NASA Contract NAS3-22055) NASA CR-165533, 1981.
16. Schmidt, C.G.; and Miller, A.K.: A Unified Phenomenological Model for Non-Elastic Deformation of Type 316 Stainless Steel—1. Development of the Model and Calculation of the Material Constants. Res. Mech., vol. 3, no. 2, Sept. 1981, pp. 109-129.
17. Chaboche, J.L.; and Rousselier, G.: On the Plastic and Viscoplastic Constitutive Equations—Part 1: Rules Developed With Internal Variable Concept. J. Pressure Vessel Technol., vol. 105, no. 2, May 1983, pp. 153-158.
18. Estrin, Y.; and Mecking, H.: A Unified Phenomenological Description of Work Hardening and Creep Based on One-Parameter Models. Acta Metall., vol. 32, no. 1, 1984, pp. 57-70.
19. Krempl, E.; McMahon, J.J.; and Yao, D.: Viscoplasticity Based on Overstress With a Differential Growth Law for the Equilibrium Stress. Mech. Mater., vol. 5, no. 1, Mar. 1986, pp. 35-48.
20. Lowe, T.C.; and Miller, A.K.: Modeling Internal Stresses in the Nonelastic Deformation of Metals. J. Eng. Mater. Technol., vol. 108, no. 4, Oct. 1986, pp. 365-373.
21. Anand, L.; and Brown, S.: Constitutive Equations for Large Deformations of Metals at High Temperatures. Constitutive Models of Deformation, J. Chandra and R.P. Srivastav, eds., SIAM, Philadelphia, 1987, pp. 1-26.
22. Perzyna, P.: Fundamental Problems in Viscoplasticity. Advances in Applied Mechanics, vol. 9, R. Von Mises and T. Von Karman, eds., Academic Press, 1966, pp. 243-377.
23. Chan, K.S., et al.: A Survey of Unified Constitutive Theories. Nonlinear Constitutive Relations for High Temperature Application—1984, NASA CP-2369, 1984, pp. 1-23.
24. Lemaitre, J.; and Chaboche, J.L.: Mecanique des Materiaux Solides. Dunod, Paris, 1985, pp. 253-341.
25. Swearengen, J.C.; and Holbrook, J.H.: Internal Variable Models for Rate-Dependent Plasticity: Analysis of Theory and Experiment. Res. Mech., vol. 13, no. 2, 1985, pp. 93-128.
26. Onsager, L.: Reciprocal Relations in Irreversible Processes I. Phys. Rev., vol. 37, no. 4, Feb. 15, 1931, pp. 405-426.
27. Germain, P.; Nguyen, Q.S.; and Suquet, P.: Continuum Thermodynamics. J. Appl. Mech., vol. 50, no. 4b, Dec. 1983, pp. 1010-1020.
28. Onat, E.T.; and Leckie, F.A.: Representation of Mechanical Behavior in the Presence of Changing Internal Structure. J. Appl. Mech., vol. 55, no. 1, Mar. 1988, pp. 1-10.
29. Freed, A.D.: Structure of a Viscoplastic Theory. NASA TM-100794, 1988.
30. Chaboche, J.L.: Time-Independent Constitutive Theories for Cyclic Plasticity. Int. J. Plast., vol. 2, no. 2, 1986, pp. 149-188.
31. Zener, C.; and Hollomon, J.H.: Plastic Flow and Rupture of Metals. Trans. ASM, vol. 33, 1944, pp. 163-235.
32. Rice, J.R.: Inelastic Constitutive Relations for Solids: An Internal-Variable Theory and Its Application to Metal Plasticity. J. Mech. Phys. Solids, vol. 19, no. 6, Nov. 1971, pp. 433-455.
33. von Mises, R.: Mechanik der festen Korper im Plastisch-Deformablen Zustand. Nachr. Ges. Wiss., Goettingen, Math. Phys. Kl., 1913, pp. 582-592.
34. Prager, W.: Recent Developments in the Mathematical Theory of Plasticity. J. Appl. Phys., vol. 20, no. 3, Mar. 1949, pp. 235-241.
35. Armstrong, P.J.; and Frederick, C.O.: A Mathematical Representation of the Multiaxial Bauschinger Effect. CEGB Report RD/B/N731, Central Electricity Generating Board, Dec. 1966.
36. Il'yushin, A.A.: On the Relations Between Stresses and Small Deformations in Mechanics of Continuous Media. PMM J. Appl. Math. Mech., vol. 18, 1954, pp. 641-666.
37. Phillips, A.: A Review of Quasistatic Experimental Plasticity and Viscoplasticity. Int. J. Plast., vol. 2, no. 4, 1986, pp. 315-328.
38. Bailey, R.W.: Note on the Softening of Strain-Hardening Metals and Its Relation to Creep. J. Inst. Met., vol. 35, 1926, pp. 27-40.
39. Orowan, E.: The Creep of Metals. J. West Scotl. Iron Steel Inst., vol. 54, 1947, pp. 45-96.
40. Freed, A.D.; and Verrilli, M.J.: A Viscoplastic Theory Applied to Copper. NASA TM-100831, 1988.
41. Marquis, D.: Modelisation et Identification de L'ecrouissage Anisotrope des Metaux. Ph.D. Thesis, Universite Pierre et Marie Curie, Paris, France, 1979, pp. 64-73.
42. Walker, K.P.; and Jordan, E.H.: Constitutive Modelling of Single Crystal and Directionally Solidified Superalloys. Turbine Engine Hot Section Technology 1987, NASA CP-2493, 1987, pp. 299-301.
43. Odqvist, F.K.G.: Mathematical Theory of Creep and Creep Rupture. 2nd ed., Clarendon Press, Oxford, London, 1974, pp. 20-35.
44. Lee, D.; and Zaverl, F., Jr.: A Generalized Strain Rate Dependent Constitutive Equation for Anisotropic Metals. Acta Metall., vol. 26, no. 11, Nov. 1978, pp. 1771-1780.
45. Miller, A.K.: A Unified Phenomenological Model for the Monotonic, Cyclic, and Creep Deformation of Strongly Work-Hardening Materials. Ph.D. Thesis, Stanford University, 1975, pp. 36-41.

46. Barrett, C.R.; and Sherby, O.D.: Steady-State Creep Characteristics of Polycrystalline Copper in the Temperature Range of 400° to 950 °C. Trans. AIME, vol. 230, no. 6, Oct. 1964, pp. 1322-1327.
47. Dorn, J.E.: Some Fundamental Experiments on High Temperature Creep. J. Mech. Phys. Solids, vol. 3, 1954, pp. 85-116.
48. Garofalo, F.: An Empirical Relation Defining the Stress Dependence of Minimum Creep Rate in Metals. Trans. AIME, vol. 227, no. 2, Apr. 1963, pp. 351-356.
49. Nix, W.D.; and Gibeling, J.C.: Mechanisms of Time-Dependent Flow and Fracture of Metals. Flow and Fracture at Elevated Temperatures, R. Raj, ed. ASM, Metals Park, OH, 1985, pp. 1-63.
50. Lamba, H.S.; and Sidebottom, O.M.: Cyclic Plasticity for Nonproportional Paths: Part 2—Comparison With Predictions of Three Incremental Plasticity Models. J. Eng. Mater. Technol., vol. 100, no. 1, Jan. 1978, pp. 104-111.
51. Krieg, R.D.: A Practical Two Surface Plasticity Theory. J. Appl. Mech., vol. 42, no. 3, Sept. 1975, pp. 641-646.
52. Dafalias, Y.F.; and Popov, E.P.: A Model of Nonlinearly Hardening Materials for Complex Loading. Acta Mech., vol. 21, no. 3, 1975, pp. 173-192.
53. Ziegler, H.: A Modification of Prager's Hardening Rule. Q. Appl. Math., vol. 17, no. 1, Apr. 1959, pp. 55-65.
54. Mroz, Z.: On the Description of Anisotropic Workhardening. J. Mech. Phys. Solids, vol. 15, no. 3, May 1967, pp. 163-175.
55. Robinson, D.N.; and Ellis, J.R.: A Multiaxial Theory of Viscoplasticity for Isotropic Materials. Turbine Engine Hot Section Technology—1986, NASA CP-2444, 1986, pp. 283-291.
56. Taylor, G.I.; and Quinney, H.: The Plastic Distortion of Metals. Phil. Trans. R. Soc. London, Ser. A, vol. 230, 1932, pp. 323-362.

NASA
National Aeronautics and Space Administration

Report Documentation Page

1. Report No.	2. Government Accession No.	3. Recipient's Catalog No.
NASA TP-2845		

4. Title and Subtitle	5. Report Date
Thermoviscoplastic Model With Application to Copper	December 1988
	6. Performing Organization Code

7. Author(s)	8. Performing Organization Report No.
Alan D. Freed	E-4280
	10. Work Unit No.
	505-63-31

9. Performing Organization Name and Address	11. Contract or Grant No.
National Aeronautics and Space Administration Lewis Research Center Cleveland, Ohio 44135-3191	
	13. Type of Report and Period Covered
	Technical Paper

12. Sponsoring Agency Name and Address	14. Sponsoring Agency Code
National Aeronautics and Space Administration Washington, D.C. 20546-0001	

15. Supplementary Notes

16. Abstract

A viscoplastic model is developed which is applicable to anisothermal, cyclic, and multiaxial loading conditions. Three internal state variables are used in the model: one to account for kinematic effects, and the other two to account for isotropic effects. One of the isotropic variables is a measure of yield strength, while the other is a measure of limit strength. Each internal state variable evolves through a process of competition between strain hardening and recovery. There is no explicit coupling between dynamic and thermal recovery in any evolutionary equation, which is a useful simplification in the development of the model. The thermodynamic condition of intrinsic dissipation constrains the thermal recovery function of the model. Application of the model is made to copper, and cyclic experiments under isothermal, thermomechanical, and nonproportional loading conditions are considered. Correlations and predictions of the model are representative of observed material behavior.

17. Key Words (Suggested by Author(s))	18. Distribution Statement
Viscoplasticity; Creep; Plasticity; Thermomechanical test; Nonproportional test	Unclassified – Unlimited Subject Category 39

19. Security Classif. (of this report)	20. Security Classif. (of this page)	21. No of pages	22. Price*
Unclassified	Unclassified	17	A03

NASA FORM 1626 OCT 86

*For sale by the National Technical Information Service, Springfield, Virginia 22161

NASA-Langley, 1988